Journal of Optoelectronics and Advanced Materials Vol. 4, No. 1, March 2002, p. 93 - 98

QUANTUM EFFICIENCY OF PHOTOINDUCED DEFECT CREATION IN AMORPHOUS As_2Se_3 FILMS

Meherun-Nessa, K. Shimakawa, A. Ganjoo

Department of Electrical and Electronic Engineering, Gifu University,
Gifu 501-1193, Japan

The quantum efficiency (QE) of photoinduced defect creation in amorphous As_2Se_3 with bandgap and sub-bandgap illumination has been deduced by using photocurrent measurements. The QE decreases with increasing number of absorbed photons, which can be explained by the rate equation for defect creation. The effect of structural flexibility on QE is also discussed.

(Received 15 March 2002; accepted 18 March 2002)

Keywords: Amorphous chalcogenide, Photoinduced defect, Quantum efficiency, Structural flexibility

1. Introduction

Absorption of bandgap or sub-bandgap light induces various changes on the structural and electronic properties of amorphous chalcogenides (a-Ch). These can be related to flexible nature of structural networks in a-Ch. The flexible or deformable structural network in amorphous semiconductors facilitates photoinduced effects to occur [1]. The photoinduced changes can be affected by varying the deposition conditions, mainly the angle of deposition, i.e., oblique deposition of the films, which results in the films having a columnar structure and a lesser density of atoms. It has been shown that the density of atoms in the films deposited obliquely at an angle of 80^o is nearly half of the normally deposited films. The lower density of atoms in obliquely deposited films results in a porous structure, with many voids between the atoms and lot of "free space". The presence of "free space" results in giant changes in bandgap and volume, when illuminated with band gap light [2, 3].

On the other hand, photoinduced defect creation occurs in a-Ch during illumination and this induces changes in electronic transport properties. Biegelsen et al. [4], by studying electron spin density of chalcogenide glasses, observed that prolonged exposure to strongly absorbed light induces a large density of metastable defects. Shimakawa et al. [5,6] also observed the similar result for defect creation while studying the photoconductivity in a-Ch. However, all kinetic equations proposed so far have discussed the time evolution light induced metastable defects (LIMD) [1] and the quantum efficiency (QE) of has not been discussed yet.

In the present study, the quantum efficiency of LIMD creation as a function of total number of absorbed photons is estimated and these results can be explained by the rate equation for defect creation. It is of interest to know how QE depends on n_p and on the photon energy in the LIMD creation. We also discuss the effect of structural flexibility on QE. To observe the effect of structural flexibility, we have studied LIMD creation during illumination by measuring photocurrent with time for normal and obliquely deposited a-As_2Se_3 films.

Table 1. Fitting parameters α, τ, N_s/N_0, and γ at 300 K and 250 K for various deposition conditions for bandgap and sub - bandgap illumination. Notations of sample are the same as in Fig. 1.

Sample (Measured temperature)	Illumination type	α	τ (s)	N_s/N_0	γ
O (300K)	Bandgap	0.80	55	1.80	0.64
O (250K)		0.90	105	4.58	0.82
N (300K)		0.90	55	1.25	0.56
N (250K)		0.96	210	4.14	0.81
O (300K)	Sub-gap	0.65	1000	0.28	0.22
O (250K)		0.65	2300	0.32	0.24
N (300K)		0.66	1300	0.15	0.13
N (250K)		0.71	2100	0.26	0.21

2. Experimental

Thin films (thickness d ~ 0.5-1 μm) of amorphous As_2Se_3 (a-As_2Se_3) were prepared onto corning 7059 glass substrates by thermal evaporation in a vacuum of ~ 2×10^{-6} Torr at room temperature. Two types of depositions (oblique and normal) were performed. Normal deposition means that the substrate is placed parallel to the source of the evapration. The oblique films were deposited with an angle of 80^0 between the normal to the substrate and the direction of the incidence of the evaporated atoms. Planar gap-cell electrodes using gold (40 μm gap separation and 5mm gap width) were fabricated onto the films. For band gap and sub-band gap illumination, the samples were illuminated with semiconductor diode lasers (hν = 1.9 eV, power = 50 mW/cm^2: G = 5×10^{20} cm^{-3}s^{-1}, and hν = 1.55 eV, power = 100 mW/cm^2: G = 4×10^{18}cm^{-3}s^{-1}) to induce photocurrent. These measurements are performed after thermal annealing the samples at 160 ^{o}C for 2 hr in a vacuum of ~ 2×10^{-6} Torr.

3. Results and discussion

Fig. 1 (a) and (b) show the experimentally obtained photocurrent I_p as a function of exposure time t at 300 K and 250 K for bandgap and sub-bandgap illuminations, respectively. The symbols used are described in the figure caption. The solid lines are calculated results, which will be discussed later. For bandgap illumination, the photocurrent I_p decreases with time and approaches a minimum and then increases for both the obliquely and normally deposited films. In obliquely deposited films I_p is comparatively lower than for normally deposited films. For sub-bandgap illumination, no pronounced decrease in I_p is observed. I_p decreases very slowly, and does not show any increase even after two hours of illumination as in the case of band gap illumination. A decrease in photocurrent could result from the photoinduced creation of recombination centers [5, 6].

In a microscopic model for LIMD creation, Shimakawa et al. [1, 5] proposed that the creation of widely separated random pairs (RPs) of positively and negatively charged centres is responsible for the decrease in the photocurrent. Such RPs result from defect-conserved bond-switching (DCBS) reactions at optically induced intimate pairs (IPs). For sub-bandgap illumination (Fig. 1(b)), we may expect that the number of RP center is smaller, resulting in a smaller decrease of I_p.

We should discuss the increase in photocurrent I_p for band gap illumination. In Fig. 1 (a) increasing component of photocurrent may be due to some structural changes taking place in the films with illumination. The increase in photocurrent can be caused by the increase of optical absorption due to photodarkening (PD), which can be responsible for the increase in the number of photo-excited carriers. The magnitude of the change of increasing photocurrent at 250 K is greater than that at 300 K, suggesting that the PD at 250 K is bigger than at 300 K. This is in accordance with the recent findings of illumination-time and temperature dependence of PD in amorphous chalcogenides [7].

Band gap light is more effective than sub-band gap light in producing PD. For sub-bandgap illumination in Fig. 1(b), even after two hours of illumination there is no increase in photocurrent.

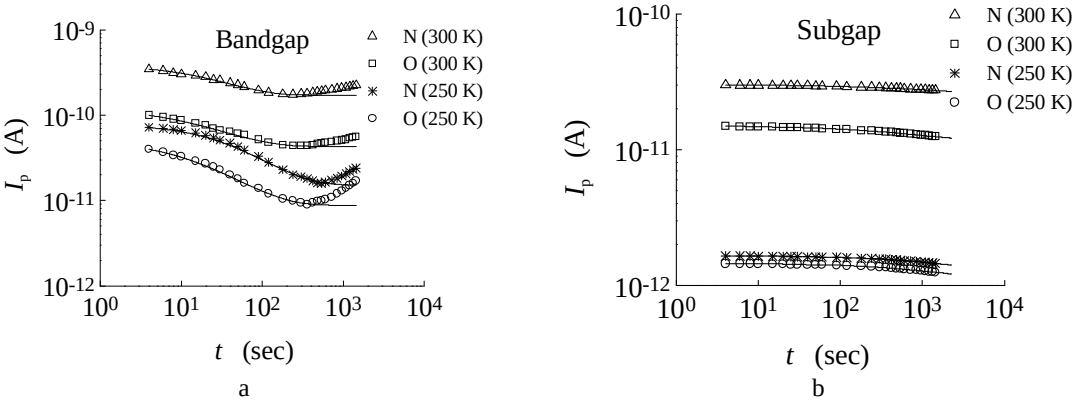

Fig. 1 Variation of photocurrent with exposure time measured at 300K and 250K for a-As_2Se_3 films for (a) bandgap illumination, and (b) sub-bandgap illumination. The symbols, □ and represent the photocurrents for obliquely deposited films measured at 250 and 300K, respectively. We denote these as O(250K) and O(300K). Δ and ∗ represent the photocurrents for normally deposited films measured at 300 and 250 K, respectively. We denote these as N(300 K) and N (250 K). Solid curves are calculated results using Eq. (4) in the text.

Now we discuss the defect creation N_t during illumination. It is assumed here that the change in the photocurrent is dominated by LIMD creation itself. The photocurrent, under conditions of thermal equilibrium, with exposure time can be expressed as

$$I_p(t) = \frac{C}{N_0 + N_t} = \frac{C}{N_0(1 + N_t / N_0)} = \frac{I_p(0)}{1 + N_t / N_0}, \tag{1}$$

where C is a constant and $I_p(0)$ (= C/N_0) is the initial photocurrent. N_t/N_0 can be estimated from the ratio $I_p(0)/I_p(t)$, with N_0 being the initial number of defects in the film. Fig. 2 (a) and (b) show the variation of defect creation (N_t/N_0), for bandgap and subgap illuminations, respectively, with exposure time estimated from the changes in photocurrent using Eq. (1). All symbols are described in the figure caption. The solid lines are calculated results, which will be discussed later. N_t increases with time during illumination in obliquely and normally deposited films. It is clear that N_t for obliquely deposited films is always larger than that for normally deposited ones at the same temperature. From this observation it is suggested that the LIMD creation is more enhanced in obliquely deposited samples than in normally deposited ones. Large structural flexibility in obliquely deposited films may show large LIMD creation.

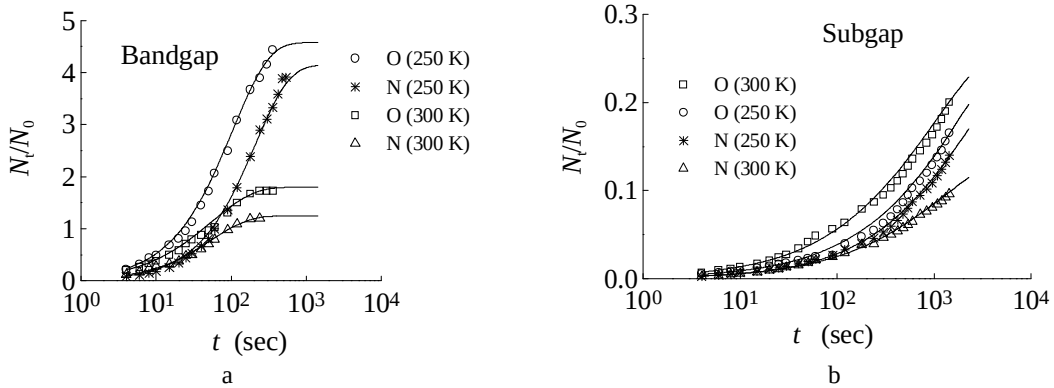

Fig. 2. Variation of N_t/N_0 with exposure time, which is estimated from the changes in photocurrent using Eq. (1) in the text for (a) bandgap and (b) subgap illumination. Description of symbols is the same as in Fig. 1. Solid lines are the fitting obtained using Eq. (3).

The rate equation for LIMD creation can be written as

$$\frac{dN_t}{dt} = k_p(N_T - N_t) - k_r N_t \tag{2}$$

where N_T is the total potential sites for LIMD creation, k_p and k_r being the promotion and recovery rate, respectively [1]. Assuming a time dispersive reaction for promotion and recover reactions as $k_p = At^{\alpha-1}$ and $k_r = Bt^{\alpha-1}$, respectively, where A and B are constant, the number of defects, N_t created during illumination is given as

$$N_t = N_s\left[1-\exp\left\{-\left(\frac{t}{\tau}\right)^{\alpha}\right\}\right], \tag{3}$$

where $N_s = N_T A/(A+B)$ is the saturated density of N_t and $\tau = [\alpha/(A+B)]^{1/\alpha}$ is the effective creation time. Here the dispersion parameter α $(0 < \alpha < 1)$ is assumed to be the same for both the forward and backward reactions. From Eq. (3) we can evaluate N_t/N_0 [dividing Eq. (3) by N_0] as a function of illumination time by taking N_s/N_0 as the fitting parameter.

Using Eqs. (1) and (3) the photocurrent can be written as

$$I_p = \frac{I_s}{1-\gamma\exp\left\{-(t/\tau)^{\alpha}\right\}}, \tag{4}$$

where I_s is a constant current reached by prolonged illumination and $\gamma = N_s/(N_0 + N_s)$.
The solid lines in Figs. 1 and 2 are calculated results by using α, τ, and N_s/N_0 (or γ) as the fitting parameters. The fittings to the experimental data are reasonably good and these parameters are tabulated in the table. This leads to the following conclusions: For both the bandgap and sub-bandgap illuminations, and for the same temperature at which illumination was made, the values of N_s/N_0 and γ for the obliquely deposited samples are larger than those for the normal ones. The effective creation time τ for the sub-bandgap illumination is larger than that for the bandgap illumination and it increases with decreasing temperature.

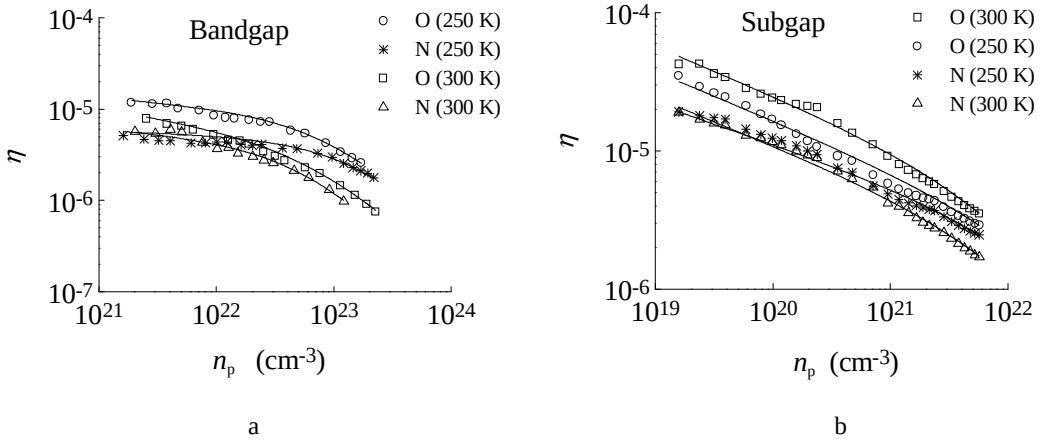

Fig. 3. Variation of quantum efficiencies η with the number of absorbed photon n_p, for (a) bandgap and (b) sub-bandgap illumination. Description of symbols is the same as in Fig. 1. Solid lines are calculated results using Eq. (5) in the text.

Finally we define the quantum efficiency η of LIMD creation, which is defined as

$$\eta = N_t / n_p , \tag{5}$$

where N_t is the number of defects created by illumination and n_p is the total number of absorbed photons. To get N_t we need to know the value of N_0. Here, the value of N_0 is assumed to be 1×10^{17} cm^{-3} [1]. The total number of absorbed photons n_p is evaluated as $n_p = Gt$, where t is the illumination time and G is the rate of absorbed photons (cm^{-3} s^{-1}). Fig. 3 (a) and (b) show the quantum efficiency η as a function of total number of absorbed photons n_p, where again symbols are described in the figure caption. It is shown that the quantum efficiency decreases with increasing number of absorbed photons for both the bandgap and sub-bandgap illumination. At the studied temperatures, all the results show a similar behavior. The solid lines in Fig. 3 (a) and (b) represent the calculated results of quantum efficiency using Eq. (3) and (5), which are also in good agreement with the experimental results. Fig. 4(a) and (b) show the comparison of quantum efficiencies in obliquely and normally deposited films for band gap and sub band gap illumination at studied temperatures (300 K, 250 K). All symbols used are described in the figure caption. At 300K the variation of quantum efficiency with number of absorbed photons is nearly parallel to each other for both band gap and sub-band gap illumination (Fig. 4 (a)), but at 250K this variation is not clear (Fig. 4 (b)).

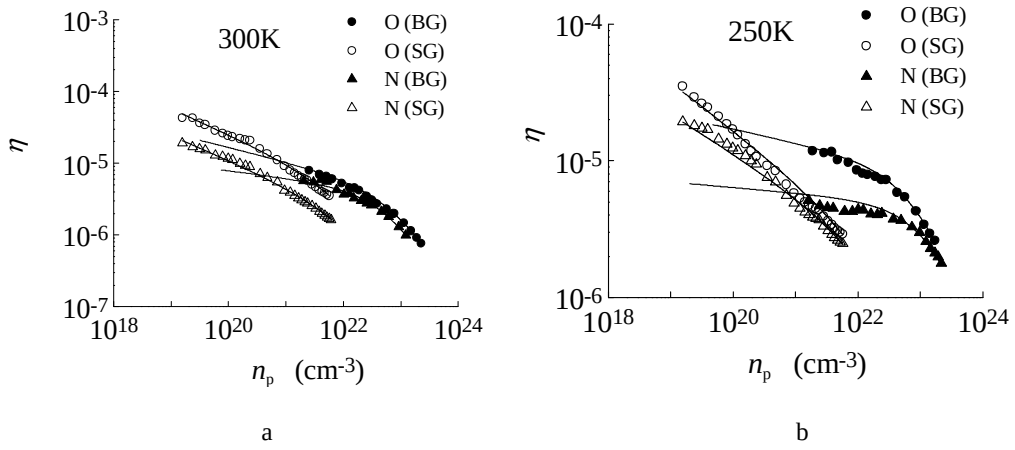

Fig. 4. Comparison of quantum efficiencies for band gap and sub-band gap illumination for obliquely and normally deposited films at (a) 300 K and (b) 250 K. The solid and open symbols represent the band gap and sub-band gap illumination, respectively (O for obliquely deposited and Δ for normally deposited films). Solid lines is the same as in Fig. 3.

From Fig. 4, it seems that at smaller n_p QE for subgap illumination is larger by a factor of 2-3 than that for bandgap illumination. This is somewhat surprising as we expect intuitively that QE for higher photon energy is larger than for lower photon energy. However, at larger n_p, the QE for subgap illumination is smaller than that for bandgap one, which agrees with the intuitive expectation. More detailed study should be required to clarify this.

5. Conclusions

We have studied the effect of structural flexibility on photoinduced defect creation in obliquely and normally deposited films of amorphous As_2Se_3, at different temperatures by band gap and sub-band gap illumination. It has been observed that the defect creations with illumination are larger for obliquely deposited films compared to normally deposited films, which may be due to a

larger flexibility of obliquely deposited films with many voids. We observed a large value of quantum efficiency even for subgap illumination.

References

[1] K. Shimakawa, A. Kolobov, S. R. Elliot, Adv. Phys. **44**, 533 (1995).
[2] A. Ganjoo, N. Yoshida, K. Shimakawa, Recent Research Developments in Applied Physics, edited by M. Kawasaki, N. Ashgriz, and R. Anthony (Research Signpost, Trivandrum, 1998) p.129.
[3] Y. Kuzukawa, A. Ganjoo, K. Shimakawa, Y. Ikeda, Phil. Mag. **B79**, 249 (1999).
[4] D. K. Biegelsen, R. A. Street, Phys. Rev., Lett. **44**, 803 (1980).
[5] K. Shimakawa, S. Inami, S. R. Elliot, Phys. Rev. **B 42**, 11857 (1990).
[6] K. Shimakawa, S. Inami, T. Kato, S. R. Elliott, Phys. Rev. **B46**, 10062 (1992).
[7] A. Ganjoo, K. Shimakawa, H. Kamiya, E. A. Davis, Jai Singh, Phys. Rev. **B**, **62**, R14601 (2000).